*Evaluation of Particle Swarm Optimization Techniques Applied to Maximum Power Point Tracking in PV systems

David Díaz Martínez[1], Rafael Trujillo Codorniu[2], Roberto Giral*[3] and Luis Vázquez Seisdedos[4]

[1]*Dept. Automática, Fac. Ing. Eléctrica, Universidad de Oriente, Santiago de Cuba, Cuba, ddiaz@uo.edu.cu*
[2]*Dept. Automática, Fac. Ing. Eléctrica, Universidad de Oriente, Santiago de Cuba, Cuba, rtrujillo@uo.edu.cu*
[3]*Dept. Eng. Electrònica, Elèctrica i Automàtica, Universitat Rovira i Virgili, Tarragona, Spain, roberto.giral@urv.cat; *Corresponding author*
[4]*Dept. Automática, Fac. Ing. Eléctrica, Universidad de Oriente, Santiago de Cuba, Cuba, lvazquez@uo.edu.cu*

Abstract

Even with significant progresses in the maximum power point (MPP) research area, the necessity to improve the existing methods becomes mandatory to increase the energy conversion efficiency. Since the power–voltage (P-V) characteristic curve of photovoltaic (PV) arrays has multiple peaks under partially shaded (PS) conditions, the conventional maximum power point tracking (MPPT) control methods have the difficult challenge of locate the global MPP (GMPP) among many local MPPs (LMPPs). In recent years, numerous research papers have been focused on techniques to efficiently track the GMPP and alleviate the partial shading effects. One of the most popular evolutionary search technique is Particle Swarm Optimization (PSO) that provides high tracking speed and the ability operate under different environmental conditions. For solving some conventional PSO technique common weaknesses, several modifications and improvements have emerged in the past years. This paper provides a comparative and comprehensive review of some relevant PSO-based methods taking into account the effects of important key issues such as particles initialization criteria, search space, convergence speed, initial parameters, performance with and without Partial Shading, and efficiency. The simulation results are validated under numerous test conditions using MATLAB code and Simulink package.

Keywords: Maximum Power Point Tracking, Particle Swarm Optimization, Partial Shading, Global peak, Bio-Inspired.

1 Introduction

Increasing demand for energy, depletion of fossil fuels and environmental pollution has motivated researchers to work in the field of renewable power generation. Solar, wind, tidal, and biomass energies have penetrated the electric power production market in recent years. [1]. Among renewables, solar energy is a competitive source of electricity growing fast mainly because of no fuel cost, low maintenance requirement, abundant availability of solar energy and pollution free.

Unfortunately, the Power-Voltage (P-V) characteristics of the solar cell is a nonlinear curve, that changes depending on irradiation and temperature. A maximum power point tracker (MPPT) is used to operate the PV array at its optimal power point, called Maximum Power Point (MPP). In large PV systems, some of the modules could receive less irradiation due to shades of surrounding trees, buildings or clouds. This called partially shaded condition (PSC) reduces the PV power output and also causes multiple MPPs in the P–V curve, i.e. one global MPP (GMPP) and several local MPPs (LMPPs). There is a significant power loss due to these multiple peaks.

Two approaches are generally used to reduce the shading effect. The first one is based on (complex and costly) hardware fixtures [2] and the second is to track the MPPT by developing advanced control algorithms. To date, several MPPT algorithms have been implemented, among them, Perturb and Observe (P&O), Incremental Conductance (InCond) and Hill-Climbing (HC) are widely in use because their simplicity of implementation and reduced complexity. Also, Fractional Short Circuit Current/Open Circuit Voltage [3], Sliding Mode Control (SMC) [4], Mathematical-Graphical Approach and Ripple Correlation Control (RCC) [5] are well known. In normal condition, i.e. uniform irradiation, they are capable of tracking the MPP quite efficiently with good convergence speed. Despite these advantages, each of these methods inherit continuous oscillation that occurs around the MPP. The oscillatory behavior results in considerable loss of power during steady state. Numerous works are carried out to minimize the oscillation, but it is achieved at the expense of reduced tracking speed [6]. However, none of these techniques are capable of handling partial shading condition, they cannot differentiate between a LMP and the GMP, leading to power losses. [7]

To solve these shortcomings, artificial intelligence (AI) approaches like Fuzzy Logic Control **(**FLC**)** [8] and Artificial Neural Network (ANN**)** [9] based techniques have been developed. Although these methods are effective in dealing with the nonlinear characteristics of the P–V curve, they require extensive computation, large amount of data required for training or depends on prior system knowledge.

Alternatively, bio-inspired algorithms are proved to be very efficient in dealing with non-linear and stochastic problems without excessive mathematical computations. Some of the bio-inspired methods are proposed in literature are: Ant Colony Optimization (ACO) [10], Particle Swarm Optimization (PSO), Genetic Algorithm

(GA) [11], Cuckoo Search [12], Flashing Firefly [13], Artificial Bee Colony (ABC) [14] and Grey Wolf Optimization (GWO) [15]. Even though these methods provide good solutions, they faced serious issues like procedural complexity, large number of parameters to be tuned and weak exploitation process.

PSO is widely accepted among these methods for tracking MPP because of its simple structure, parallel processing, good robustness, easy implementation, fast computation capability and high probability of finding the global optimal solution. The metaheuristic approach of this method makes it independent of the output characteristics of PV systems. Because of its good performance in multiple-peak functions optimization, PSO is very suitable for MPPT control of PV systems under PSC [16]. Although the PSO method introduces higher possibilities to reach global peak under shading conditions, the convergence to the optimal operating region is not always guaranteed.

Several PSO-based MPPT algorithms have been developed for PV systems to solve the multiple local MPP problem. Deterministic PSO (DPSO) [17], Adaptive Perceptive PSO (APPSO) [18], Improved PSO (IPSO) [19] [20] and Modified Swarm optimization (MPSO) [21], [22] are some of the more notable research woks.

Several hybrid methods with good performance have been presented. In one hand, with traditional methods; PSO-Hill-Climbing [19], PSO-P&O in [23], PSO-InCond in [24].

By other hand, hybrid PSO-AI techniques are also popular; A PSO-ANN algorithm was proposed in [25] to detect the global peak. An optimization of a FLC-based MPPT algorithm using PSO is presented in [26]. Authors in [27] presents a new scheme which combines the basic PSO with the grouping idea of Shuffled Frog Leaping Algorithm (SFLA) to divide the particle population into multiple group/swarms. A hybrid Differential Evolution-PSO method called DEPSO is shown in [28].

However, two particular issues of the PSO based MPPT algorithm are the long tracking time toward the MPP within large search spaces [17] and the random numbers used in standard PSO formulation that could reduce the searching efficiency. Conventional PSO can track the GMP under time-invariant PS patterns efficiently and accurately. Once the GMP changes due to time-variant Shading Pattern, PSO sticks to the first GMP and becomes unable to catch the dynamic GMP without certain initialization or particles [29]. The initialization of the swarm is an essential factor that affects the effectiveness of PSO. The method in general, requires parameter tuning and good initial values to avoid premature convergence.

This paper is devoted to analyze some of the most significant modifications of a standard PSO (non-including hybrid techniques) and compare the influence of parameters tuning in the performance, capacity to find global maximum, dynamic response, efficiency and tracking speed.

This paper is structured as follows. A PV energy system modelling is given in section 2. The PSO structure and studied methodologies are shown in Section 3. Section 4 discusses and analyzes the simulations. Finally, Section 5 provides conclusions.

2. PV Modeling

In general, single diode and double diode models [30] are the two ways followed in literature for modelling PV panels. The double diode model is accurate when compared to a single diode model [31] but requires more parameters to model accurately the solar PV array, hence, the single diode model is selected for simplicity. The PV cell equivalent circuit (Figure 1) can be represented by a current source connected in parallel to a diode [32].

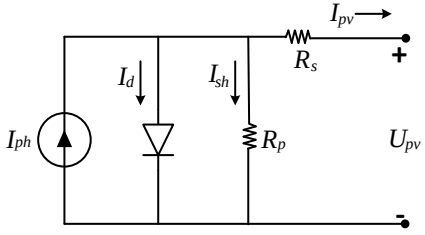

FIGURE 1 A single diode model of solar PV.

The output current of the module can be determined by Equation 1:

$$I = I_{ph} - I_o \left[exp\left(\frac{V_{pv}+I_{pv}R_s}{vT}\right) - 1 \right] - \frac{V_{pv}+I_{pv}R_s}{R_p} \quad (1)$$

where I_o is the diode saturation current, R_s is series resistance, R_p is shunt resistance, vT is the modified diode ideality factor $[\{vT = N_s akT\}/q]$, q- electron charge ($1.6 \cdot 10^{-19}\ C$), k- Boltzmann constant, a- diode ideality constant, Ns– number of series connected cells, T-operating temperature (25 °C), I_{pv} and V_{pv} are the output current and voltage respectively, and I_{ph} is the photocurrent (2):

$$\mathrm{I_{ph}} = \mathrm{I_{ph_{ref}}}[1 + \alpha'_{\mathrm{T}}(\mathrm{T} - \mathrm{T_{ref}})]\frac{\mathrm{G}}{\mathrm{G_{ref}}} \quad (2)$$

were G is irradiation, α'_T is the relative temperature coefficient of short-circuit current and all ref terms are related to Standard Reference Condition (SRC) $[G_{ref} = 1000\ W/m^2, T_{ref} = 25\ ℃]$.

The PV selected to perform the comparisons is a commercial HELIENE, model HEE215MA68. The parameters of this module are listed in Table 1.

TABLE 1 Specifications for Heliene HEE215MA68

Electrical Characteristics	HEE215MA68
Open Circuit Voltage ($\boldsymbol{V_{oc}}$)	37.40 V
Short Circuit current ($\boldsymbol{I_{sc}}$)	8.72 A
Maximum Power voltage ($\boldsymbol{V_{mpp}}$)	30.30 V
Maximum power current ($\boldsymbol{I_{mpp}}$)	8.22 A
Maximum power ($\boldsymbol{P_{mmp}}$)	250 W
$\boldsymbol{I_{sc}}$ temperature coefficient	0.07 A/°C
$\boldsymbol{V_{oc}}$ temperature coefficient	-0.34 V/°C

3. General overview of conventional PSO

PSO was introduced by James Kennedy and Russell C. Eberhart in 1995 [33]. It is a population based stochastic optimization technique used to determine the required parameters by maximizing the objective function in a given search space. Compared with many evolutionary algorithms, PSO normally provides faster convergence speed. The PSO based tracking systems do not require any derivatives calculation, also have low number of tuning parameters, system independency, high probability of finding the global optimal solution and high computational efficiency.

Taking inspiration from flocking behavior of birds, N_p particles are used to search for the maximum or minimum values of an objective function. The particles are randomly initialized and start to move in a given search space with a certain velocity. Then, for each iteration, a new velocity value is calculated based on the current velocity, the previous best position and the global best position. Later, the new position is updated by using the previous position and the new velocity value. During this optimization process, the agents are spread over the search space in different directions.

The velocity of i^{th} particle is denoted by v_i, represents the step size and is calculated as:

$$\mathrm{v_i^{k+1}} = \mathrm{w v_i^k} + \mathrm{c_1 r_1}\left\{\mathrm{P_{best_i}} - \mathrm{x_i^k}\right\} + \mathrm{c_2 r_2}\left\{\mathrm{G_{best}} - \mathrm{x_i^k}\right\}, \tag{3}$$

and the position of i^{th} particle, x_i, is adjusted using the following equation:

$$\mathrm{x_i^{k+1}} = \mathrm{x_i^k} + \mathrm{v_i^{k+1}} \tag{4}$$

Here w is the inertia weight, c_1 and c_2 are the acceleration coefficients, r_1 and r_2 are random numbers in the range (0-1), P_{best_i} is the personal best position of particle i, and G_{best} is the best position of the particles. (3) and (4) are called flight equations and shows that the new position of each particle is affected by three terms. The first term, inertia weight ω, is the current velocity of the particle. The second term, weighted by cognitive acceleration coefficient c_1, prompts the attraction of the particle towards its own personal best (cognition influence) and the third term,

weighted by social acceleration coefficient c_2, prompts the attraction of the particle towards the global best (social influence). The personal best position P_{best_i} is updated using Eq. (5) if the condition in Eq. (6) is satisfied, i.e.

$$\mathrm{P_{best_i}}=x_i^k \tag{5}$$

$$\mathrm{f(x_i^k) > f(P_{best_i})} \tag{6}$$

where ''f'' is the objective function (operating power of the PV array).
The described processes are repeated until the termination criterion is satisfied. The flowchart of basic PSO is shown in Figure 2 and the operating principle can be described as follows [34]:

Step 1 (PSO Initialization): Particles are usually initialized randomly over the search space. Initial velocities are taken randomly.
Step 2 (Fitness Evaluation): Evaluate the fitness value of each particle. This is conducted by supplying the candidate solution to the objective function.
Step 3 (Update Best Data): Individual and global best fitness values (P_{best_i} and G_{best}) are updated by comparing the newly calculated fitness values against the previous ones, and replacing the P_{best_i} and G_{best} as well as their corresponding positions as necessary.
Step 4 (Update Velocity and Position): The velocity and position of each particle in the swarm are updated using (3) and (4).
Step 5 (Convergence Determination): Check the convergence criterion. If the convergence criterion is met, the process can be terminated; otherwise, the iteration number will increase by 1 and go to step 2

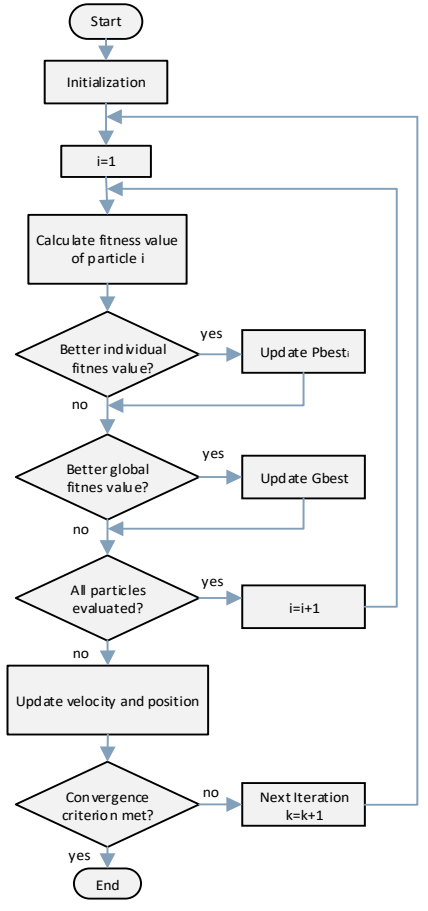

FIGURE 2 Flow diagram of PSO

The search efficiency and success rate of PSO are determined primarily by the values assigned for the weights and the learning factors (w, c_1 and c_2) [35]. Even the slight change in their values may lead to the variation of tracking speed and accuracy. When the weight is too high, the particle search might lack accuracy because the movement step sizes are too large. However, if the weight is low, particle movement becomes slow, and the local optimum trap might be unavoidable when facing multipeak values. In this behavior is also important the influence of random numbers in the last two terms in velocity equation (r_1 and r_2). Thus, the random nature of standard PSO could be a problem for some situations.

PSO for MPPT [36]

Here, a PSO algorithm is applied to track the MPP using the direct control technique. In order to start the optimization, a solution vector of duty cycles with N_p particles needs to be defined as follows:

$$x_i^k = d = [d_1, d_2, d_3, \dots\dots\dots, d_i] \tag{7}$$

$$i = 1, 2, \dots\dots\dots, N_p \quad \text{number of particles}$$

N_p is chosen in order to ensure the optimization of the convergence process. Numerous experimental studies have found that the optimal commitment between accuracy and convergence speed is achieved with 3 particles. This value is used by authors analyzed in next sections and thus, will be employed in this work for simulations.

The objective function can be formulated as follows:

$$P(d_i^k) > P(d_i^{k-1}) \tag{8}$$

where P is the PV power, d is the duty cycle, i is the number of particles and k is the iteration number.

Reinitialization condition

The PSO approach is usually implemented to resolve problems for which the best solution is time invariant. In this context, however, the fitness value, MPP, is frequently changed depending on the environment and load conditions. These circumstances require the re-initialization of particles in order to look for the new MPP. Considering the change in irradiation and shading pattern to be detected, the particles will be reinitialised whenever the following constraint is satisfied:

$$\frac{\left|P_{pv_{new}} - P_{pv_{last}}\right|}{P_{pv_{last}}} \geq \Delta P(\%) \tag{9}$$

where $P_{pv_{new}}$ is the new PV power, $P_{pv_{last}}$ is the PV power of the last operating point and $\Delta P(\%)$ is the normalised power tolerance. Its tipical value in literature is set to 10 % or selected as 0.1. Thus, if the normalized power mismatch is larger than 0.1, the samples will be dispersed on the PV curve and the tracking will be initialized again; otherwise they remain on the MPP.

Next, some of the relevant modifications to standard PSO proposed in literature are analized.

Deterministic PSO (DPSO) [17]

As discussed previously, dependence on random numbers (r_1, r_2) in eq. 3 could lead to tracking difficulties. However, it can be resolved by observing in P–V curves under PSC that the minimum distance between two consecutive peaks are displaced by 80% of the V_{oc} of the unshaded module. Thus, by removing the random factor in (3) and limiting the velocity factor (v_{max}) according to the distance between two peaks, the conventional PSO is transformed to a more deterministic structure. The modified velocity equation of PSO can be written as:

$$v_i^{k+1} = wv_i^k + \{P_{best_i} - x_i^k\} + \{G_{best} - x_i^k\} \quad \text{or}$$
$$v_i^{k+1} = wv_i^k + \{P_{best_i} + G_{best} - 2x_i^k\} \tag{10}$$
$$\text{for} \quad 0 < v < v_{max}$$

The tuning effort is reduced since only the inertia weight (w) needs to be tuned. The searching capability tends to be slower, but the GP tracking is guaranteed. Taking $v_{max} = 0.035$ ensures that no major peak is missed.

The stopping condition occurs when the change in the velocity of any particle d_i, reaches a (predefined) small value and the difference between the voltage of d_i particle to other particles d_j is sufficiently small ($i \neq j$). The difference could be selected between 30 % and 60 % of v_{oc_module}.

Accelerated PSO (APSO) [16]

The particle with the highest fitness value is perturbed by a P&O algorithm so that the best particle moves faster to the global MPP, and at the same time attracts the remaining particles to converge toward it more quickly. Hence, the search time needed for convergence could be significantly reduced. Additionally, there is no need to add any constraint on the optimal particle velocity. The proposed strategy can improve MPPT effectiveness without adding any additional complexity.

Also, in this proposed APSO method, there is no need to search for local best. So, Equation (3) can be modified to (11), and the convergence of the algorithm only depends on the Gbest. Furthermore, the new equation will reduce the calculation complexity:

$$v_i^{k+1} = wv_i^k + \beta\{G_{best} - x_i^k\} \tag{11}$$

So, the new particle position can be determined as Equation (12):

$$x_i^{k+1} = wv_i^k + (1-\beta)x_i^k + \beta G_{best} \tag{12}$$

where β = 0.1–0.7

The initial particles are placed on fixed positions. The first particle is set as 10% of the PV open circuit voltage (V_{oc}) and the third particle is set as 90% of V_{oc}. These particles defined the PSO search space. The intermediate particle is randomly set within this range.

Modified PSO (MPSO) [22]

In this study, consistent decreases of the weighting factor and cognitive and social parameters are adopted reducing the steps in each iteration. Greater step sizes are used to increase the particle search velocity during the initial search because the distance to the global optimum is relatively large initially. This prevents an excessively small step size from making local optimum traps unavoidable.

$$\mathrm{w(k)} = \mathrm{w_{max}} - \frac{\mathrm{k}}{\mathrm{k_{max}}}(\mathrm{w_{max}} - \mathrm{w_{min}}) \tag{13}$$

$$\mathrm{c_1(k)} = \mathrm{c_{1max}} - \frac{\mathrm{k}}{\mathrm{k_{max}}}\left(\mathrm{c_{1max}} - \mathrm{c_{1min}}\right) \tag{14}$$

$$\mathrm{c_2(k)} = \mathrm{c_{2max}} - \frac{\mathrm{k}}{\mathrm{k_{max}}}(\mathrm{c_{2max}} - \mathrm{c_{2min}}) \tag{15}$$

The particles are ititializated around a definite point in the searching space between $[d_{min}\ d_{max}]$. Two convergence criteria are employed. The method will terminate if the maximum number of iterations is attained or if all the particles' velocities become smaller than a certain threshold.

Weighting PSO (WPSO) [35]

The PSO algorithm proposed in this study involves modifying the weighting of the conventional PSO. Specifically, Equation (16) is used to adjust the basic weighting and apply larger particle movements during the early iterations; this enables transcending of regional optimal solutions.

$$\mathrm{w} = \mathrm{w_{max}} - \left((\mathrm{w_{max}} - \mathrm{w_{min}})\mathrm{x}\left(\frac{\mathrm{k}}{\mathrm{n}}\right)^2\right) \tag{16}$$

The power feedback method is adopted to examine the slope (m) and changes in power (ΔP) of the P–V curve (Figure 3) of a PV array. Table 2 lists the criteria for adjusting the weighting value. Specifically, $\Delta w = [(w_{max} - w_{min})/2]/11$ is used as the reference value for increasing or decreasing the weighting value, which is linearly adjusted according to the 11 ranges of the P–V curve slope indicated in Table 2. Values of m and ΔP are defined using Equations (17) and (18).

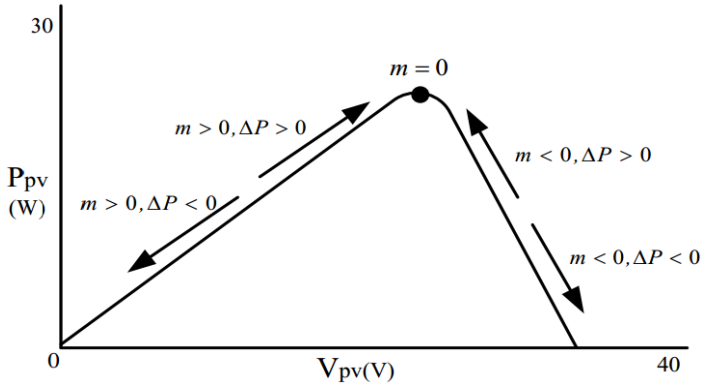

FIGURE 3 Slope (*m*) and changes in power (*ΔP*) of the P–V curve

$$\mathrm{m} = \frac{\mathrm{P}_{(\mathrm{k}+1)} - \mathrm{P}_{(\mathrm{k})}}{\mathrm{v}_{(\mathrm{k}+1)} - \mathrm{v}_{(\mathrm{k})}} \tag{17}$$

$$\Delta \mathrm{P} = P_{(k+1)} - P_{(k)} \tag{18}$$

TABLE 2 Weigthing value adjustment according to the slope and changes in *ΔP*

Condition	$\boldsymbol{m = \frac{P_{(k+1)} - P_{(k)}}{v_{(k+1)} - v_{(k)}}}$	**ΔP > 0**
1	$m > 2$	W+3ΔW
2	$2 \geq m > 1.5$	W+2ΔW
3	$1.5 \geq m > 1$	W-ΔW
4	$1 \geq m > 0.5$	W-2ΔW
5	$0.5 \geq m > 0$	W-3ΔW
6	$m = 0$	W
7	$0 > m \geq -0.5$	W-3ΔW
8	$-0.5 > m \geq -1$	W-2ΔW
9	$-1 > m \geq -1.5$	W-ΔW
10	$-1.5 > m \geq -2$	W+2ΔW
11	$m < -2$	W+3ΔW

By other hand, Equation (19) decreases cognition learning factor c_1 as the iteration number increases, indicating reduced reference to individual optimal locations. By contrast, Equation (20) increases social learning factor c_2 as the iteration number increases, indicating that reliance on the global optimal location is increased.

$$\mathrm{c}_1(\mathrm{k}) = \mathrm{c}_{1\max} - \left(\mathrm{c}_{1\max} - \mathrm{c}_{1\min}\right)\left(\frac{\mathrm{k}}{\mathrm{k}_{\max}}\right)^2 \tag{19}$$

$$\mathrm{c}_2(\mathrm{k}) = \mathrm{c}_{2\min} + \left(\mathrm{c}_{2\max} - \mathrm{c}_{2\min}\right)\left(\frac{\mathrm{k}}{\mathrm{k}_{\max}}\right)^2 \tag{20}$$

Differential PSO (DiPSO) [37]

The additional feature of this method is considering the opinion of one of the particles selected randomly from the swarm. The randomly-scaled difference of the particle and its opinion-giver particle is included in the velocity equation of the particle necessary to escape from local minima, thus the MPP can be obtained much sooner than using the classical PSO. Mathematically, the concepts of DiPSO can be expressed as follows:

$$v_{i,j}^{k+1} = wv_{i,j}^{k} + C_1 r_1 \left\{P_{best_{i,j}} - x_{i,j}^{k}\right\} + C_2 r_2 \left\{G_{best} - x_{i,j}^{k}\right\} + C_3 r_3 \left\{x_{h,j}^{k} - x_{i,j}^{k}\right\} \quad (21)$$

c_3 is the scaling factor, whereas h represents the expert particle corresponding to target particle i. In this equation, h varies from 1 to n but $h \neq i$. Scaling factor c_3 is assumed to be 0.04.

4. Study cases and simulation results

Programming and simulations were carried out in MATLAB/SIMULINK environment. The simulated system consists of PV array connected to a resistive load through a boost converter with MPPT controller, as depicted in Figure 4. The component parameter values for the converter circuitry are given in Table 3. Sample time is set to 0.1 s.

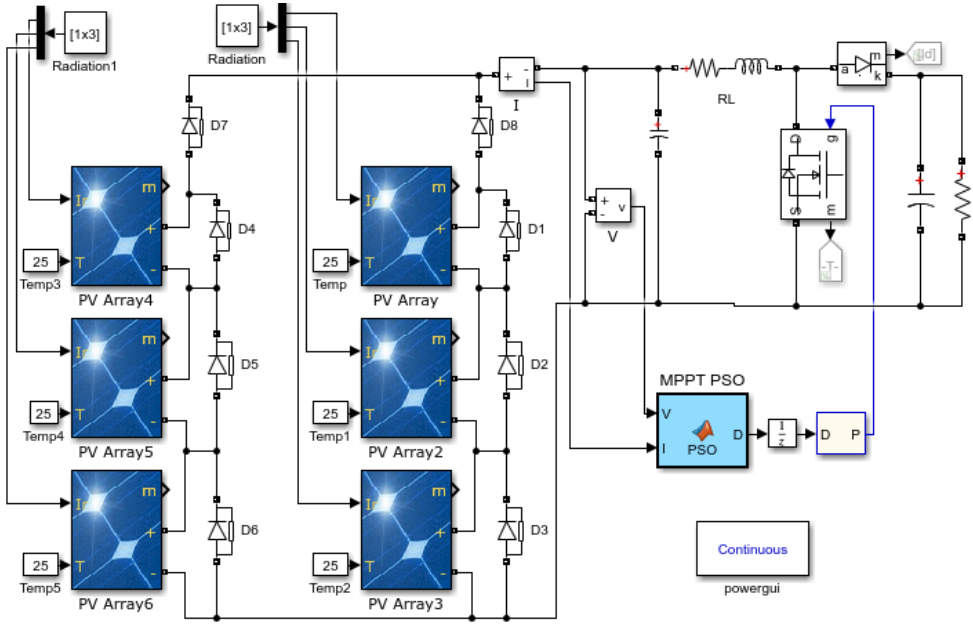

FIGURE 4 Simulink diagram of a PV system with boost converter and MPPT controller

in a 3S2P array configuration

TABLE 3 Rated configuration values of the boost converter.

Component	Value
Inductor (L)	1 mH
Capacitor (Cin)	470 µF
Capacitor (Cout)	220 µF
Switching frequency (f)	20 kHz
Sampling Time	0.1 s

All MPPT algorithms used in this paper have been tested for a number of particles (N_p=3) and the maximum and minimun duty clycle values have been set to d_{min}=0.2 and d_{max}=0.9. The rest of specific parameters for each method are listed in Table 4.

TABLE 4 Parameters configuration for all PSO techniques

	PSO	**DPSO**	**WPSO**	**DiPSO**	**MPSO**	**APSO**
$\boldsymbol{n}$	3	3	3	3	3	3
$\boldsymbol{k}$	15	15	15	15	15	15
$\boldsymbol{w}$	0.5	0.4	-	0.5	-	0.4
$\boldsymbol{w_{min}}$	-	-	0.2	0.1	0.1	-
$\boldsymbol{w_{max}}$	-	-	0.9	0.5	1	-
$\boldsymbol{C_1}$	1.5	-	-	1.5	-	-
$\boldsymbol{C_2}$	1.5	-	-	2.5	-	1.5
$\boldsymbol{C_{1min}}$	-	-	0.9	-	1	-
$\boldsymbol{C_{1max}}$	-	-	1.5	-	1.2	-
$\boldsymbol{C_{2min}}$	-	-	0.9	-	1	-
$\boldsymbol{C_{2max}}$	-	-	1.5	-	1.6	-

In order to show the MPPT performances obtained through the proposed techniques, different PV arrays configurations were considered, consisting on 6 or 8 PV modules connected in series-parallel: 3S2P and 4S2P (Figure 6). Each module is connected in parallel to a bypass diode and each series branch has anti-return diode. Numerical simulations have been carried out for different Partial Shading (PS) patterns, subjecting the PV system to challenging scenarios. The simulation study also includes the transient response when the shading pattern changes from one to another and simulation results are presented with a comparison.
For all these shading cases, dynamic power tracking experiments were conducted (in the interest of limiting paper length, dynamic response plots are not shown here),

and the corresponding total power injected into the load are summarized in Tables 5 and 6 (in bold best values, and local peaks in underlined italic).

During simulation, all the methods are compared with the same operating conditions. This is essential, since the efficiency of the proposed methods is judged based on this comparison. Throughout the experiment, the temperature is maintained constant at 25∘C.

In the first test situation, both PV array configurations receive uniform irradiation. Different steps are introduced as the simulation proceeds. $G = 1000\ \mathrm{W/m^2}$ at t=0 sec, $G = 400\ \mathrm{W/m^2}$ at t=6.5 sec and $G = 800\ \mathrm{W/m^2}$ at t=13 sec.

Another set of 3 simulations are now carried out on the 3S2P configuration, where the respective partial shading patterns and P-V curves are given in Figure 5a. In each pattern, the global maximum is located in different sections of the P-V curve to submit the system to complex operating conditions: each pattern has 3 peaks located at right, middle and left side of the P-V curve respectively. Irradiation values for each pattern are show in Figure 6a.

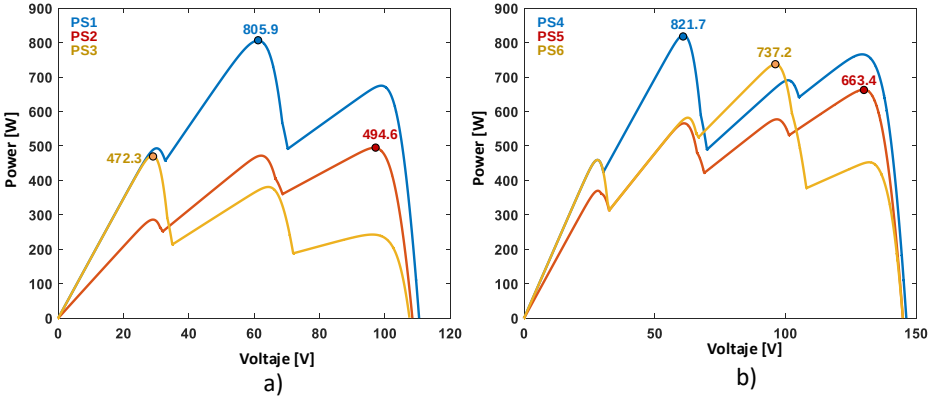

FIGURE 5 P-V curves originated from Partial Shading Conditions.
a) 3S2P array config. b) 4S2P array config.

The last set of simulations are carried out with the 4S2P configuration. Figs. 5b and 6b-6f shows corresponding P-V curves and irradiation values. Four peaks are now found in each pattern, also in different places of the searching space. The P–V characteristics of a PV array get more complex under partially shaded conditions and bear multiple peaks

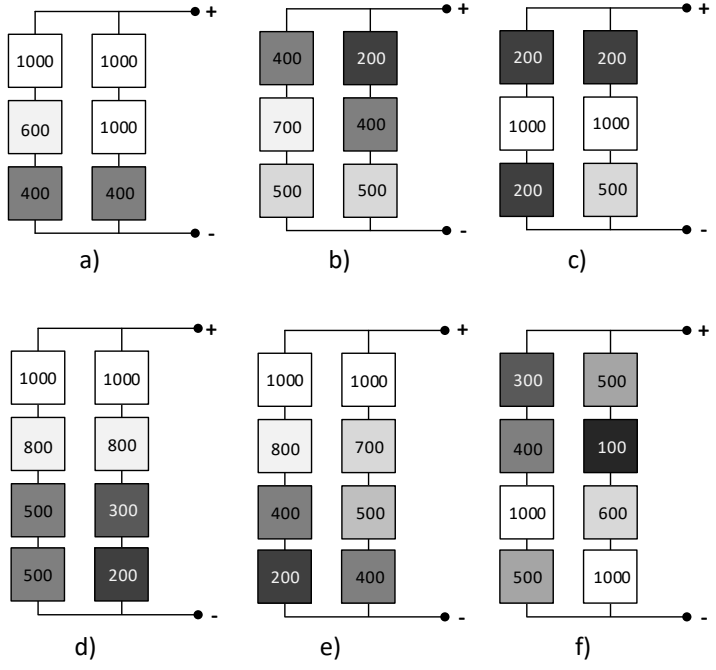

FIGURE 6 Irradiation levels [W/m2] over PV modules for Partial Shading Condition
a) PS1 b) PS2 c) PS3 d) PS4 e) PS5 f) PS6

The values of power generated were further analyzed by its tracking efficiency according to (22) as below.

$$\text{Tracking efficiency, } \mathrm{n} = \frac{\mathrm{P_{mpp}}}{\mathrm{P_{max}}} \mathrm{x}\, 100 \tag{22}$$

where P_{mpp} is the averaged output power obtained under steady state and P_{max} is the maximum available power of the PV module under a certain shading pattern. Under fast transient changes in irradiation, the system should sense these changes, execute the reinitialization command, and find the new MPP. In the corresponding simulation, the MPPT program starts execution with uniform irradiation $\mathrm{G} = 1000\ \mathrm{W/m^2}$. At 6.5 sec of simulation time, a rapid drop in irradiation is observed to $\mathrm{G} = 400\ \mathrm{W/m^2}$. Finally, at 13 sec, irradiation rises to $\mathrm{G} = 800\ \mathrm{W/m^2}$, which again results in the reinitialization command and tracks the new MPP.

3S2P array configuration

From fig. 5, values of global (P_g) and local peaks (P_L) are:

PS1: $P_g = 805.98$ W, $P_{L1} = 674.9$ W, $P_{L2} = 493.1$ W
PS2: $P_g = 494.62$ W, $P_{L1} = 471.8$ W, $P_{L2} = 285.9$ W
PS3: $P_g = 472.39$ W, $P_{L1} = 380.8$ W, $P_{L2} = 326.2$ W

Results discussion

It can be observed from Table 5, that in the three uniform irradiation conditions, all methods were able to find the MPP. In all cases, the best results are DPSO and WPSO with the best precision performance in a short tracking time. Some variations can be found analyzing partial shading patterns. In PS1, PSO and DiPSO presented the highest value of power generated, although all came to the MPP with great precision, except for P&O who stay stucked in a local maxima of 674.06 W.

Similar situation occurs in PS2, but this time is APSO the only method that cannot reach the global peak (GP), staying in a local peak (LP) at 471.49 W. The best results are provided by PSO and DPSO.

By other hand, PS3 provides a very difficult situation in which six of the methods stay at local peaks and only APSO is capable to find the MPP.

TABLE 5. Performance results for 3S2P array configuration

Pattern	Method	Time [s]	Pmax [W]	Efficiency [%]	SS Error [W]
Uniform 1000 [W/m^2]	P&O	3.41	1493.64	99.830	2.55
	PSO	3.41	1495.65	99.964	0.538
	DPSO	3.64	**1495.98**	99.987	0.201
	WPSO	**2.53**	**1496.03**	99.990	0.152
	DiPSO	3.18	1495.63	99.964	0.535
	MPSO	4.50	1458.95	97.511	37.239
	APSO	**2.89**	1495.78	99.973	0.406
Uniform 400 [W/m^2]	P&O	**1.82**	601.83	99.948	0.315
	PSO	2.44	601.78	99.939	0.366
	DPSO	3.21	**602.05**	99.984	0.098
	WPSO	2.85	**602.09**	99.990	0.058
	DiPSO	2.31	601.74	99.939	0.365
	MPSO	3.65	601.89	99.958	0.254
	APSO	**1.36**	599.33	99.532	2.819

Uniform 800 [W/m^2]	P&O	**1.50**	1202.63	99.864	1.640
	PSO	3.58	1203.95	99.974	0.314
	DPSO	**2.11**	**1204.12**	99.988	0.144
	WPSO	**2.79**	**1204.12**	99.988	0.147
	DiPSO	3.48	1203.91	99.973	0.323
	MPSO	3.63	1203.80	99.961	0.465
	APSO	3.44	1202.18	99.827	2.088
PS1	P&O	1.52	*674.096*	83.636	131.88
	Standard	4.42	**805.866**	99.985	0.118
	DPSO	3.91	805.833	99.981	0.152
	WPSO	4.33	805.786	99.975	0.199
	DiPSO	4.45	**805.867**	99.985	0.118
	MPSO	**3.61**	805.863	99.985	0.122
	APSO	**2.72**	804.712	99.842	1.273
PS2	P&O	**0.87**	494.181	99.909	0.449
	PSO	4.05	**494.444**	99.962	0.186
	DPSO	**2.32**	**494.579**	99.990	0.051
	WPSO	3.04	493.324	99.736	1.306
	DiPSO	4.10	**494.442**	99.962	0.187
	MPSO	3.94	494.352	99.944	0.278
	APSO	3.22	*471.493*	95.322	23.137
PS3	P&O	**0.09**	*325.964*	69.003	146.42
	PSO	**1.70**	*390.994*	82.770	81.393
	DPSO	4.20	*380.656*	80.581	91.734
	WPSO	**1.7**	*390.994*	82.769	81.396
	DiPSO	1.91	*390.997*	82.770	81.393
	MPSO	3.12	*391.000*	82.771	81.390
	APSO	2.11	**471.971**	99.911	0.419

4S2P array configuration

For uniform irradiation, all methods find the MPP with slight differences in maximum power. Best results are provided by PSO and DPSO, very closely followed by WPSO and DiPSO.

For partial shading (Table 6), in PS4, only DPSO and APSO are capable to find P_g at 821.7 W. The rest stay at local maximum (765.9 W) at the right of P-V curve.

From figure 5, values of global (P_g) and local peaks (P_L) are:

PS4: $P_g = 821.72$ W, $P_{L1} = 765.9$ W, $P_{L2} = 690.8$ W, $P_{L3} = 549.3$ W
PS5: $P_g = 663.43$ W, $P_{L1} = 577.3$ W, $P_{L2} = 565.6$ W, $P_{L3} = 369.8$ W
PS6: $P_g = 737.27$ W, $P_{L1} = 582.0$ W, $P_{L2} = 459.2$ W, $P_{L3} = 452.5$ W

TABLE 6. Performance results for 4S2P array configuration

Pattern	Method	Time [s]	Pmax [W]	Efficiency [%]	SS Error [W]
Uniform 1000 [W/m^2]	P&O	3.03	1991.76	99.844	3.111
	PSO	3.72	1994.66	99.990	0.195
	DPSO	**2.77**	**1994.79**	99.996	0.086
	WPSO	4.25	**1994.77**	99.995	0.100
	DiPSO	3.28	1994.69	99.991	0.186
	MPSO	3.11	1975.04	99.006	19.831
	APSO	**1.58**	1993.94	99.953	0.932
Uniform 400 [W/m2]	P&O	**2.06**	802.362	99.940	0.481
	PSO	3.33	**802.787**	99.993	0.056
	DPSO	2.43	802.745	99.988	0.098
	WPSO	2.75	802.693	99.981	0.150
	DiPSO	2.68	**802.787**	99.993	0.056
	MPSO	3.94	802.774	99.991	0.069
	APSO	**2.34**	801.961	99.890	0.882
Uniform 800 [W/m^2]	P&O	**1.72**	1603.93	99.894	1.708
	PSO	3.54	**1605.47**	99.990	0.161
	DPSO	3.24	**1605.52**	99.993	0.117
	WPSO	3.21	1605.39	99.985	0.245
	DiPSO	3.43	**1605.48**	99.990	0.161
	MPSO	3.71	1603.29	99.854	2.348
	APSO	**2.01**	1605.11	99.967	0.528
PS4	APSO	**0.42**	*765.535*	93.162	56.186
	PSO	3.11	*765.689*	93.181	56.032
	DPSO	4.52	**821.384**	99.959	0.337
	WPSO	**2.53**	*765.824*	93.198	55.897
	DiPSO	3.14	*765.690*	93.181	56.031
	MPSO	3.32	*765.888*	93.205	55.833

	APSO	**2.71**	**821.590**	99.984	0.1310
PS5	P&O	**0.15**	662.745	99.896	0.693
	PSO	**2.30**	650.013	97.976	13.425
	DPSO	3.90	**663.352**	99.987	0.086
	WPSO	**2.09**	662.541	99.865	0.897
	DiPSO	3.23	662.541	99.865	0.897
	MPSO	3.31	**663.085**	99.947	0.353
	APSO	**2.3**	650.013	97.976	13.425
PS6	P&O	**0.15**	735.247	99.725	2.027
	PSO	3.64	737.195	99.989	0.079
	DPSO	**2.31**	734.530	99.628	2.743
	WPSO	3.60	**737.209**	99.991	0.064
	DiPSO	3.61	**737.198**	99.990	0.075
	MPSO	3.33	728.574	98.820	8.699
	APSO	3.63	737.153	99.984	0.121

In PS5 and PS6 all methods get the global maximum, nevertheless, the best results in maximum power value achieved in PS5 are provided by DPSO and MPSO, and, in PS6, by WPSO and DiPSO.

DiPSO results are very similar to standard PSO in all cases, except in PS5, so, it does not represent any significant variation with respect to the standard PSO method.

Although P&O finds global maxima successfully in all uniform irradiation conditions, it fails and is trapped at local peaks in three cases of partial shading: PS1, PS3 and PS4. This shortcoming is because of its inability to discriminate between uniform and partial shading conditions.

Some of the conventional methods are typically configured to start at the middle of the search space, which attunes them to finding the GMPP under certain conditions. Following this, in this work, the initial value of the duty cycle (D_0) for the P&O method has been set to 0.5.

Table 7 compares the results of the P&O method obtained using (D_0=0.5) with those obtained for D_0 = 0.7. Local peaks have been highlighted in underlined italic. It is clear that in some cases, a value of D_0=0.7 yields local maxima, while in other cases offers a better performance than D_0=0.5 in achieving global maxima. There are also some situations for which both initial values are inadequate.

Selecting the most appropriate initial values depend on the shape of the P-V curve and on how far the corresponding initial generated power is from the global peak. This is the reason why in some circumstances, when the peak is near, P&O finds the MPP very quickly but fails in other cases.

TABLE 7 Performance of different duty cycles initial values for P&O method (t [s] and Pmax [W])

	PS1		PS2		PS3		PS4		PS5		PS6	
D	t	Pmax	t	Pmax	t	Pmax	t	Pmax	t	Pmax	t	Pmax
0.5	1.5	*674*	0.8	494.2	0.1	*325.9*	0.4	*765.5*	0.2	*677.7*	0.1	662.7
0.7	2.5	804.5	0.05	*471*	0.9	*380.2*	2.3	818.6	1.4	*746*	0.9	*564.6*

Is important to note the common point on the two situations where most of the PSO-based methods present difficulties finding MPP: this point is located at the left of P-V curve. Fortunately, experiments demonstrate that this kind of shape on the P-V curve is the lees commonly caused by PS conditions. Anyway, some improvements are still needed on these methods to solve this problem.

An important performance criterion is tracking speed. Results shows that this feature is not accompanied with precision on finding MPP. P&O converge fast but fails many times staying at local peaks. Of PSO-based methods, in average, APSO is clearly the leader. Here, the convergence only depends on global best G_{best}, since the local best term P_{best} was removed from the velocity equation. Thus, the simplicity of the algorithm makes it very fast. Second position is for WPSO. Even behind standard PSO, the slower method was MPSO, who also turns out to be the worst in tracking precision.

Despite being the oldest of the analyzed modified methods, best overall performance is provided by DPSO. Except for PS3, it was capable to find successfully the MPP in a reasonably short time with very high precision over 99.95 %. Proposed by Ishaque back in 2013, it continues being a powerful approach. Limited v_{max} ensures that no major peak is missed. Although this constraint limits the searching capability, its transformation to a more deterministic structure by removing random numbers actually reduces tracking time.

Also remarkable was the behavior of APSO and WPSO, despite APSO was the only one stucked at a local peak in PS2, in other complex circumstances like PS3 and PS4 when others fail, its performance was notorious in finding MPP accurately and very fast.

Similar in strategy than APSO, WPSO uses a different approach by increasing social learning factor c_2 when learning factor c_1 decreases and therefore providing more independence of individual optimal locations and more reliance on the global optimal location as iteration number increases. In addition, variable weighting is key factor, in this case guided by equations (17) and (18) according to position of MPP in the P-V curve. Large speed when the particle is far from MPP and reduced movement when it is close are required for accurately tracking.

CONCLUSIONS

The dynamic responses of two different configurations, 3S2P and 4S2P, of small PV systems to six PSO-based MPPT methods have been studied using a MATLAB simulation scheme comprising a digital controller, a Boost converter, and a PV array that includes bypassing diodes. The MPP tracking performances were verified in different atmospheric conditions, both for uniform irradiation and partial shading, following similar procedures to those reported in the literature.

Compared to P&O, the analyzed PSO methods significantly improve the reliability and effectiveness of the MPPT for the PV system under PS conditions in terms of converging to the MPP accurately and reducing the output power oscillations. Steady-state efficiency on average is always above 99.75 %.

Of the analyzed techniques, the most outstanding in average efficiency for all types of atmospheric conditions is DPSO. On the other hand, APSO is the fastest in finding the MPP. Both methods highlight in these two performance criteria, efficiency and speed of tracking, over the other techniques.

Since the studied PSO-based methods are mathematically simple, it is straightforward to deduce that they will be easily implemented in low-cost microcontrollers. Future works will verify that these PSO-based tracking schemes offer a feasible alternative solution for adoption in commercial MPPT controllers.

Acknowledgements

"This contribution is a result of a cooperation with Automatic Control and Industrial Electronics Group (GAEI) from University Rovira i Virgili with Power Electronics Control in Energy and Motion Systems group (PECEM) from University of Oriente, and the IRIS project (Cuban energy transformation. Integration of Renewable Intermittent Sources in the power system) finnanced by Academy of Science from Finland. The authors of the article gratefully acknowledge the financers and project partners"

References

[1] L. Vazquez *et al.*, "Energy System Planning towards Renewable Power System: Energy Matrix Change in Cuba by 2030," in *10th IFAC Symposium on Control of Power and Energy Systems. CPES* Tokyo, 2018, pp. 522–527: IFAC PapersOnLine 51-28.

[2] E. Koutroulis and F. Blaabjerg, "A new technique for tracking the global maximum power point of pv arrays operating under partial-shading conditions," *IEEE Journal of Photovoltaics*, vol. 55, pp. 184 –190, April 2015.

[3] H. A. Sher, A. F. Murtaza, A. Noman, K. E. Addoweesh, and M. Chiaberge, "An intelligent control strategy of fractional short circuit current maximum power point tracking technique for photovoltaic applications. ," *Journal of Renewable and Sustainable Energy*, vol. 7, 2015.

[4] K. Il-Song, "Sliding mode controller for the single-phase grid-connected photovoltaic system," *Applied Energy*, vol. 83, 2006.

[5] M. Hammami and G. Grandi, "A Single-Phase Multilevel PV Generation System with an Improved Ripple Correlation Control MPPT Algorithm," *Energies*, vol. 10, p. 2037, 2017.

[6] A. H. Mohammed *et al.*, "Comparative assessment of maximum power point tracking procedures for photovoltaic systems," *Green Energy & Environment*, vol. 5, 2017.

[7] Ali M. Eltamaly, H. M. H. Farh, and M. F. Othman, "A novel evaluation index for the photovoltaic maximum power point tracker techniques," *Solar Energy*, vol. 174, pp. 940–956, 2018.

[8] T. Kwan and X. Wu, "Maximum power point tracking using a variable antecedent fuzzy logic controller," *Solar Energy*, vol. 137, pp. 189–200, 2016.

[9] S. Duman, N. Yorukeren, and I. H. Altas, "A novel MPPT algorithm based on optimized artificial neural network by using FPSOGSA for standalone photovoltaic energy systems," *Neural Computing and Applications*, vol. 29, pp. 257– 278, 2018.

[10] S. Titri, C. Larbes, K. Y. Toumi, and K. Benatchba, "A new MPPT controller based on the Ant colony optimization algorithm for Photovoltaic systems under partial shading conditions," *Applied Soft Computing*, vol. 58, pp. 465–479 2017.

[11] A. A. S. Mohamed, A. Berzoy, and O. A. Mohammed, "Design and hardware implementation of FL-MPPT control of PV systems based on GA and small-signal analysis," *IEEE Trans. Sustainable Energy*, vol. 8, pp. 279–290, 2017.

[12] A. J and S. Z, "A maximum power point tracking (MPPT) for PV system using Cuckoo Search with partial shading capability," *Applied Energy*, vol. 119, pp. 118–130, 2014.

[13] K. Sundareswaran, S. Peddapati, and S. Palani, "MPPT of PV systems under partial shaded conditions through a colony of flashing fireflies," *IEEE Trans Energy Convers*, vol. 29, pp. 463–472, 2014.

[14] K. Sundareswaran, P. Sankar, P. Nayak, S. Simon, and S. Palani, "Enhanced energy output from a PV system under partial shaded conditions through artificial bee colony," *IEEE Trans. Sustainable Energy* vol. 6, pp. 198–209, 2015.

[15] L. P. Sampaio, M. V. da Rocha, S. A. O. da Silva, and M. H. T. de Freitas, "Comparative analysis of MPPT algorithms bio-inspired by grey wolves employing a feed-forward control loop in a three-phase grid-connected photovoltaic system,"

IET Renewable Power Generation, vol. 13, pp. 1–12, 2019.

[16] M. Alshareef, Z. Lin, M. Ma, and W. Cao, "Accelerated Particle Swarm Optimization for Photovoltaic Maximum Power Point Tracking under Partial Shading Conditions," *Energies*, vol. 12, 2019.

[17] K. Ishaque and Z. Salam, "A Deterministic Particle Swarm Optimization Maximum Power Point Tracker for Photovoltaic System Under Partial Shading Condition," *IEEE Transactions On Industrial Electronics*, vol. 60, 2013.

[18] M. Miyatake, M. Veerachary, F. Toriumi, N. Fujii, and H. Ko, "Maximum Power Point Tracking of Multiple Photovoltaic Arrays: A PSO approach," *IEEE Transactions on Aerospace and Electronic Systems*, vol. 47, pp. 367-380, 2011.

[19] K. Ishaque, Z. Salam, M. Amjad, and S. Mekhilef, "An improved particle swarm optimization (PSO)-based MPPT for PV with reduced steady state oscillation," *IEEE Trans. Power Electrononics*, vol. 27, pp. 3627–3638, 2012.

[20] K. H. Chao, Y. S. Lin, and U. D. Lai, "Improved Particle Swarm Optimization for Maximum Power Point Tracking in Photovoltaic Module Arrays.," *Applied Energy*, vol. 1158, pp. 609–618, 2015.

[21] R. Venugopalan, N. Krishnakumar, T. Sudhakarbabu, K. Sangeetha, and N. Rajasekar, "Modified Particle Swarm Optimization technique based Maximum Power Point Tracking for uniform and under partial shading condition," *Appl. Soft Computing Journal*, vol. 30, pp. 613–24, 2015.

[22] M. Abdulkadir and A. Yatim, "Optimization of an MPPT-based Controller for PV System using PSO," *European Journal of Advances in Engineering and Technology*, vol. 5, 2018.

[23] K. Sundareswaran, K. V. Vignesh, and S. Palani, "Application of a combined particle swarm optimization and perturb and observe method for MPPT in PV systems under partial shading conditions," *Renewable Energy*, vol. 75, pp. 308–17, 2015.

[24] J. Liu, J. Li, J. Wu, and W. Zhou, "Global MPPT algorithm with coordinated control of PSO and INC for rooftop PV array. ," *Journal of Engineering*, pp. 778–782, 2017.

[25] S. Z. Said, L. Thiaw, and C. W. Wabuge, "Maximum Power Point Tracking of Photovoltaic Generators Partially Shaded Using a Hybrid Artificial Neural Network and Particle Swarm Optimization Algorithm," *Int. Journal Energy Power Eng*, vol. 6, pp. 91–99, 2017.

[26] P. C. Cheng, B. R. Peng, Y. H. Liu, Y. S. Cheng, and J. W. Huang, "Optimization of a fuzzy-logic-control-based mppt algorithm using the particle swarm optimization technique. ," *Energies*, vol. 8, 2015.

[27] M. Mao, L. Zhang, Q. Duan, O. Oghorada, Q. Duan, and B. Hu, "A Two-Stage Particle Swarm Optimization Algorithm for MPPT of Partially Shaded PV Arrays," *International Journal of Green Energy*, 2017.

[28] M. Seyedmahmoudian, R. Rahmani, S. Mekhilef, and e. al., "Simulation and hardware implementation of new maximum power point tracking technique for partially shaded PV system using hybrid DEPSO method," *IEEE Trans Sustain Energy*, vol. 6, pp. 850–862, 2015.

[29] A. M. Eltamaly, H. M. H. Farh, and M. S. Al Saud, "Impact of PSO Reinitialization on the Accuracy of Dynamic Global Maximum Power Detection of Variant

Partially Shaded PV Systems," *Sustainability*, vol. 11, p. 2091, 2019.

[30] G. Petrone, C. Ramos-Paja, and G. Spagnuolo, *Photovoltaic Sources Modeling*. NJ, USA, , 2017.

[31] V. Chin, Z. Salam, and K. Ishaque, "Cell modelling and model parameters estimation techniques for photovoltaic simulator application: a review," *Applied Energy* vol. 154, pp. 500–519, 2015.

[32] H.-J. Chiu *et al.*, "A battery charger with maximum power point tracking function for low-power photovoltaic system applications," *Int. J. Circ. Theor. Appl.* , vol. 39, pp. 241–256, 2011.

[33] R. Eberhart and J. Kennedy, "A new optimizer using particle swarm theory," in *in: Proceedings of the sixth international symposium on micro machine and human science MHS '95*, New York, NY, USA, 1995, pp. 39-43.

[34] R. Thankakan and E. Samuel Nadar, "Investigation of the double input power converter with N stages of voltage multiplier using PSO-based MPPT technique for the thermoelectric energy harvesting system," *International Journal of Circuit Theory and Applications*, vol. 48, no. 3, 2019.

[35] L.-Y. Chang, Y.-N. Chung, K.-H. Chao, and J.-J. Kao, "Smart Global Maximum Power Point Tracking Controller of Photovoltaic Module Arrays," *Energies*, vol. 11, 2018.

[36] S. Rajendran and H. Srinivasan, "Simplified accelerated particle swarm optimisation algorithm for efficient maximum power point tracking in partially shaded photovoltaic systems," *IET Renewable Power Generation*, 2016.

[37] V. H. Dong, K. H. Nhu, T. T. Hoang, and T. C. Pham, "Tracking maximum power point for photovoltaic system using a novel differential particle swarm optimization," *Journal of Mechanical Engineering Research and Developments (JMERD)*, vol. 41, 2018.